

1 **ASYMPTOTIC PRESERVING SCHEMES FOR KINETIC EQUATIONS THAT**  
2 **ARE ALSO STATIONARY PRESERVING\***

3 C.EMAKO<sup>†</sup>, F.KANBAR <sup>‡</sup>, C.KLINGENBERG<sup>‡</sup>, AND M.TANG <sup>§</sup>

4 **Abstract.** In this work we are interested in the stationary preserving (SP) property of asymptotic preserving  
5 (AP) schemes for kinetic models. Our key observation is that as far as some macroscopic quantities can be updated  
6 explicitly, a large class of AP schemes have the SP property as well. To illustrate the generality of our observa-  
7 tion, three different AP schemes for three different kinetic models are considered. Their SP properties are proved  
8 analytically and tested numerically, which confirms our observations.

9 **Key words.** Asymptotic preserving, Stationary preserving, Neutron transport equation, Chemotaxis kinetic  
10 model, The Boltzmann equation, Parity based schemes, UGKS, Penalty method.

11 **AMS subject classifications.** 65M08, 35Q20, 35Q92

12 **1. Introduction.** Kinetic models describe the time evolution of probability density distribu-  
13 tion of particles that travel freely for a certain distance and then change their directions due to  
14 collision or scattering. They usually include a transport term that takes into account the move-  
15 ment of the particles and integral terms that take into account the scattering, tumbling or colliding.  
16 When the average distance between two successive velocity change is small, i.e. the mean free path  
17 is small, one has to use resolved space and time steps that are less than the mean free path. More-  
18 over, the probability density function in kinetic models depends not only on space and time but  
19 also on velocity. The high dimensionality and the small mean free path lead to an extremely high  
20 computational cost and AP schemes that allow mean free path independent meshes become popular  
21 in last decades.

22 AP schemes were first proposed in [15, 14] for the neutron transport equation and have been suc-  
23 cessfully extended to a lot of applications, we refer to the review paper [21] for more discussions.  
24 Different AP schemes have been developed for various kinetic models, including the neutron trans-  
25 port equation [1, 13, 15, 16], the velocity jump model for E.coli chemotaxis [3, 6] and the Boltzmann  
26 equation [8, 23, 4, 12].

27 The Knudsen number is the ratio of the mean free path and the domain typical length scale  
28 [14]. To prove that a scheme is AP, one has to show that when the Knudsen number goes to zero  
29 in the discretized scheme, it converges to a good discretization of the corresponding limit model.  
30 The main advantage of AP schemes is that their stability and convergence are independent of the  
31 Knudsen number. On the other hand, there are situations when in applications the solution after  
32 some time reaches a quasi-stationary state, meaning that numerically the difference between the  
33 global equilibrium and the solution after finite time is smaller than machine precision. In semi-  
34 conductor models such a state is the mode of operation of the electronic device, namely the state  
35 where the applied voltage is in equilibrium so that no current flows. Thus it is of interest to have  
36 a numerical scheme maintains stationary solutions up to machine precision. We call such schemes  
37 stationary preserving (SP).

---

\*Submitted to the editors 13.01.2020.

**Funding:** 2nd author: National Council for Scientific Research of Lebanon (CNRS-L). 2nd, 3rd author: Bay-  
risches Hochschulzentrum for China.

<sup>†</sup>Sorbonne University, UPMC Univ Paris 06, UMR 7598, Laboratoire Jacques-Louis Lions, F-75005, Paris, France.

<sup>‡</sup>University of Wuerzburg, Germany.

<sup>§</sup>Department of Mathematics and Institute of Natural Sciences, Jiao Tong Univ., Shanghai, China.

38 Our key observation is that as far as some macroscopic quantities can be updated explicitly, a  
 39 large class of AP schemes have the SP property as well. To illustrate the idea, we present here a  
 40 glimpse of the proof of the SP property for an AP scheme for the BGK model [4]. The BGK model  
 41 writes:

$$42 \quad (1.1) \quad \partial_t f + v \cdot \nabla_x f = \frac{1}{\tau} [M_f - f].$$

43 where  $f(x, v, t)$  is the probability density function at time  $t$ , position  $x$  and moving with velocity  
 44  $v$ .  $M_f$  is the Maxwellian distribution and  $\tau$  is the relaxation time. At the macroscopic level, mass,  
 45 momentum and energy are moments of the distribution function  $f$  in velocity space that are given  
 46 by:

$$47 \quad \rho(x, t) = \int_V f(x, v, t) dv,$$

$$48 \quad \rho u(x, t) = \int_V v f(x, v, t) dv,$$

$$49 \quad E(x, t) = \int_V \frac{1}{2} |v|^2 f(x, v, t) dv.$$

52 As  $\tau \rightarrow 0$ , these moments solves the Euler equations,

$$53 \quad (1.2) \quad \begin{aligned} \rho_t + \nabla \cdot (\rho u) &= 0, \\ (\rho u)_t + \nabla \cdot (\rho u \otimes u + p) &= 0, \\ E_t + \nabla \cdot ((E + p)u) &= 0. \end{aligned}$$

54 As in [8], we consider the following AP IMEX scheme

$$55 \quad (1.3) \quad \frac{f^{n+1} - f^n}{\Delta t} + v \cdot \nabla_x f^n = \frac{1}{\tau} [M_f^{n+1} - f^{n+1}].$$

56 Suppose that the solution reaches the stationary state at time  $t^n$ , i.e.  $f^n$  satisfies the following  
 57 equation:

$$58 \quad (1.4) \quad v \cdot \nabla_x f^n = \frac{1}{\tau} [M_f^n - f^n].$$

59 Multiplying (1.4) by  $\alpha(v)$  with  $\alpha(v) = (1, v, \frac{1}{2}|v|^2)$  and integrating over the velocity space leads to

$$60 \quad (1.5) \quad \int_V \alpha(v) v \cdot \nabla_x f^n = 0.$$

61 Now multiplying (1.3) by  $\alpha(v)$  and integrating over  $V$ , one gets

$$62 \quad (1.6) \quad \frac{\int_v \alpha(v) f^{n+1} - \int_v \alpha(v) f^n}{\Delta t} + \int_V \alpha(v) v \cdot \nabla_x f^n = 0.$$

63 From (1.5), the moments are preserved. The Maxwellian can be updated explicitly and it is exactly  
 64 equal to the Maxwellian at the previous time step, i.e.  $\mathcal{M}^{n+1} = \mathcal{M}^n$ . Hence, the discretized  
 65 equation can be now written as,

$$66 \quad \frac{f^{n+1} - f^n}{\Delta t} + v \cdot \nabla_x f^n = \frac{1}{\tau} [M_f^n - f^n + f^n - f^{n+1}].$$

67 Noting that  $f^n$  satisfies (1.4), thus

$$68 \quad \frac{f^{n+1} - f^n}{\Delta t} + \frac{[f^{n+1} - f^n]}{\tau} = 0,$$

69 which yields  $f^{n+1} = f^n$  and the stationary solution is preserved. Our proof of the SP property  
 70 is independent of  $\varepsilon$ . In other words no matter how small  $\varepsilon$  is, the SP property holds. In the  
 71 subsequent part, we will consider three different classes of AP schemes for which one can prove  
 72 their SP properties. To get the SP property, it is crucial to show that the macroscopic quantities  
 73 in these AP schemes are being updated explicitly, even though the schemes are implicit or IMEX.  
 74 As one can see from the SP proof, once we are able to show that the macroscopic quantities are  
 75 preserved, the SP property follows immediately. To show the universality of our observation, we  
 76 test different kinetic models for different AP schemes, as listed in Table 1.

77 The paper is structured as follows: In section 2, the parity equations-based AP scheme developed  
 78 in [21] for the neutron transport equation is considered and then the SP property of the scheme is  
 79 proved. In section 3, the unified gas kinetic scheme [16, 23, 24](UGKS) is extended to the velocity  
 80 jump chemotaxis model and then we prove that this extension has the SP property. In section 4,  
 81 we consider the penalization method proposed in [8] for the Boltzmann equation and prove its  
 82 SP property. Finally, we present some numerical results to show the AP and SP properties of  
 83 each numerical scheme in section 5. All three different strategies of developing AP schemes (Parity-  
 84 equations based scheme, UGKS, penalization method) have been extended to various kinetic models  
 85 and thus the extension of our observation is natural.

Section	Kinetic Model	Scheme
2	Neutron transport equation	Parity-equations based scheme
3	Chemotaxis kinetic model	UGKS
4	Boltzmann equation	IMEX scheme with the Penalization method

TABLE 1

*A list of kinetic models together with their corresponding schemes.*

86 **2. Parity equations-based scheme for the Neutron transport equation.** In this section  
 87 we check the Parity equations-based AP scheme for the neutron transport equation in [21, 22]. This  
 88 scheme is then proved to be SP as well.

89 **2.1. The neutron transport equation.** Consider the one-dimensional neutron transport  
 90 equation:

$$91 \quad (2.1) \quad \partial_t f + \frac{1}{\varepsilon} v \cdot \nabla_x f = \frac{\sigma_T}{\varepsilon^2} \left( \frac{1}{2} \int_{-1}^1 f dv' - f \right) - \sigma_a \left( \frac{1}{2} \int_{-1}^1 f dv' \right) + q$$

93 with  $x \in [x_L, x_R]$  and  $v \in [-1, 1]$ . We present the scheme for a simplified neutron transport equation  
 94 with  $\sigma_T = 1, \sigma_a = 0, q = 0$ . The extension to more general cases does not add any difficulties.

95 **2.2. Discretization of the model.** When  $\sigma_T = 1, \sigma_a = 0, q = 0$  in (2.1), the Parity  
 96 equations-based scheme in [22] can be summarized by the following steps:

97 • Rewrite (2.1) into two equations. For  $v \geq 0$ ,

$$\begin{aligned} \varepsilon \partial_t f(v) + v \partial_x f(v) &= \frac{1}{\varepsilon} \left( \frac{1}{2} \int_{-1}^1 f dv - f(v) \right), \\ \varepsilon \partial_t f(-v) - v \partial_x f(-v) &= \frac{1}{\varepsilon} \left( \frac{1}{2} \int_{-1}^1 f dv - f(-v) \right). \end{aligned} \quad (2.2)$$

99 • Introduce the even and odd parities that are

$$r(t, x, v) = \frac{1}{2} [f(t, x, v) + f(t, x, -v)], \quad j(t, x, v) = \frac{1}{2\varepsilon} [f(t, x, v) - f(t, x, -v)].$$

100 • Add and subtract the equations in (2.2) and rewrite them into the following diffusive  
 101 relaxation system,

$$\begin{aligned} \partial_t r + v \partial_x j &= -\frac{1}{\varepsilon^2} (r - \rho_r), \\ \partial_t j + \eta v \partial_x r &= -\frac{1}{\varepsilon^2} [j + (1 - \varepsilon^2 \eta) v \partial_x r], \end{aligned} \quad (2.3)$$

102 where  $\rho_r = \int_0^1 r dv'$  and  $\eta(\varepsilon) = \min(1, \frac{1}{\varepsilon})$ .

103 • Split the equations (2.3) into two steps:

104 – Relaxation step:

$$\begin{cases} \partial_t r = -\frac{1}{\varepsilon^2} (r - \rho_r), \\ \partial_t j = -\frac{1}{\varepsilon^2} [j + (1 - \varepsilon^2 \eta) v \partial_x r]. \end{cases}$$

105 – Transport step:

$$\begin{cases} \partial_t r + v \partial_x j = 0, \\ \partial_t j + \eta v \partial_x r = 0. \end{cases}$$

106 • Discretize the two steps as follows:

107 – For the transport step, we use an explicit first order upwind scheme on its diagonal  
 108 from such that

$$\begin{cases} r_i^{n+\frac{1}{2}} = r_i^n - v \frac{\Delta t}{\Delta x} D^u j_i^n, \\ j_i^{n+\frac{1}{2}} = j_i^n - \eta v \frac{\Delta t}{\Delta x} D^u r_i^n. \end{cases} \quad (2.4)$$

109 where  $D^u f_i^n = f_{i+1}^n - f_i^n$  and  $D^c f_i^n = \frac{f_{i+1}^n - f_{i-1}^n}{2}$  are respectively the upwind and the  
 110 central spatial differences.

111 – For the relaxation step, we use an implicit backward Euler method that writes

$$\begin{cases} \frac{r_i^{n+1} - r_i^{n+\frac{1}{2}}}{\Delta t} = -\frac{1}{\varepsilon^2} (r_i^{n+1} - \rho_{r_i}^{n+1}), \\ \frac{j_i^{n+1} - j_i^{n+\frac{1}{2}}}{\Delta t} = -\frac{1}{\varepsilon^2} (j_i^{n+1} + (1 - \varepsilon^2 \eta) v \frac{D^c}{\Delta x} r_i^{n+1}). \end{cases}$$

121 By integrating the above first equation over  $V$  we find,  $\rho_{r_i}^{n+1} = \rho_{r_i}^{n+\frac{1}{2}}$ . Then,

$$122 \quad (2.5) \quad \begin{cases} r_i^{n+1} = Ar_i^{n+\frac{1}{2}} + B\rho_{r_i}^{n+\frac{1}{2}}, \\ 123 \quad j_i^{n+1} = Aj_i^{n+\frac{1}{2}} - B(1 - \varepsilon^2\eta)v\frac{D^c}{\Delta x}r_i^{n+1}, \end{cases}$$

124 with A and B being defined as:

$$125 \quad A = \frac{\varepsilon^2}{\varepsilon^2 + \Delta t} \quad \text{and} \quad B = \frac{\Delta t}{\varepsilon^2 + \Delta t}.$$

126 The fully space-time discretized parity equations-based AP scheme is given by the transport step  
127 (2.4) and the relaxation step (2.5). The boundary conditions for  $r$  and  $j$  are the same as in [22]  
128 and are obtained using the following relations:

$$129 \quad (2.6) \quad r + \varepsilon j|_{x=x_L} = F_L(v) \quad \text{and} \quad r - \varepsilon j|_{x=x_R} = F_R(v)$$

130 when  $\varepsilon \ll 1$ ,  $j$  can be approximated by,

$$131 \quad (2.7) \quad j = -v\partial_x r$$

132 from the second equation in (2.3). Hence, the boundary conditions for  $r$  and  $j$  are (2.8) and (2.9),

$$133 \quad (2.8) \quad r - \varepsilon v\partial_x r|_{x=x_L} = F_L(v) \quad \text{and} \quad r + \varepsilon v\partial_x r|_{x=x_R} = F_R(v)$$

134

$$135 \quad (2.9) \quad j = -v\partial_x r$$

136 where  $F_L(v)$  and  $F_R(v)$  are the inflow boundary conditions of  $f$ . The AP proof of the scheme has  
137 been done in [22], [21], [3].

138 **2.3. SP Property.** We will prove that the above AP scheme is SP as well. Plugging (2.4)  
139 in (2.5) and using the fact that  $\rho_r^{n+\frac{1}{2}} = \rho_r^{n+1}$ , the equations for updating  $r^{n+1}$  and  $j_i^{n+1}$  can be  
140 written as:

$$141 \quad (2.10a) \quad \frac{r_i^{n+1} - r_i^n}{\Delta t} + v\frac{D^u}{\Delta x}j_i^n = -\frac{1}{\varepsilon^2}(r_i^{n+1} - \rho_{r_i}^{n+1}),$$

$$142 \quad (2.10b) \quad \frac{j_i^{n+1} - j_i^n}{\Delta t} + \eta v\frac{D^u}{\Delta x}r_i^n = -\frac{1}{\varepsilon^2}(j_i^{n+1} + (1 - \varepsilon^2\eta)v\frac{D^c}{\Delta x}r_i^{n+1}).$$

144 DEFINITION 2.1. A steady state solution of (2.3) is a function pair  $(r^n, j^n)$  that satisfies:

$$145 \quad v\partial_x j^n = -\frac{1}{\varepsilon^2}(r^n - \rho_r^n),$$

$$146 \quad \eta v\partial_x r^n = -\frac{1}{\varepsilon^2}[j^n + (1 - \varepsilon^2\eta)v\partial_x r^n].$$

148 with the same boundary conditions as in (2.8) and (2.9).

149 DEFINITION 2.2. A discrete stationary solution to (2.10) are  $r_i^n$  and  $j_i^n$  that satisfies:

$$150 \quad (2.11a) \quad v\frac{D^u}{\Delta x}j_i^n = -\frac{1}{\varepsilon^2}(r_i^n - \rho_{r_i}^n),$$

$$151 \quad (2.11b) \quad \eta v\frac{D^u}{\Delta x}r_i^n = -\frac{1}{\varepsilon^2}[j_i^n + (1 - \varepsilon^2\eta)v\frac{D^c}{\Delta x}r_i^n].$$

152

153 LEMMA 2.3. When  $r_i^n$  and  $j_i^n$  are discrete stationary solution that satisfies (2.11), the scheme  
 154 in (2.10) will lead to  $r_i^{n+1} = r_i^n$  and  $j_i^{n+1} = j_i^n$ . Hence the parity equations-based scheme is SP.

155 *Proof.* • For r: Since  $\rho_{r_i}^n = \int_0^1 r_i^n$ , integrating (2.11a) over  $[0, 1]$  yields

$$156 \quad (2.12) \quad \int_0^1 v \cdot \frac{D^u}{\Delta x} j_i^n dv = 0.$$

157 Integrating (2.10a) with respect to  $v$  over  $[0, 1]$  and using (2.12), one finds,

$$158 \quad \frac{\rho_{r_i}^{n+1} - \rho_{r_i}^n}{\Delta t} + \int_0^1 v \cdot \frac{D^u}{\Delta x} j_i^n dv = 0,$$

159 and thus  $\rho_r^{n+1} = \rho_r^n$ . Using (2.11a) and  $\rho_r^{n+1} = \rho_r^n$ , (2.10a) gives

$$160 \quad \frac{r_i^{n+1} - r_i^n}{\Delta t} - \frac{1}{\varepsilon^2} (r_i^n - \rho_{r_i}^n) = -\frac{1}{\varepsilon^2} (r_i^{n+1} - \rho_{r_i}^n).$$

161 Hence,

$$162 \quad \left( \frac{1}{\Delta t} + \frac{1}{\varepsilon^2} \right) (r_i^{n+1} - r_i^n) = 0.$$

163 and then  $r_i^{n+1} = r_i^n$ .

164 • For j: Using  $r^{n+1} = r^n$ , (2.10b) becomes

$$165 \quad (2.13) \quad \frac{j_i^{n+1} - j_i^n}{\Delta t} + \eta v \frac{D^u}{\Delta x} r_i^n = -\frac{1}{\varepsilon^2} [j_i^{n+1} + (1 - \varepsilon^2 \eta) v \frac{D^c}{\Delta x} r_i^n].$$

166 From (2.11b), (2.13) writes,

$$167 \quad \frac{j_i^{n+1} - j_i^n}{\Delta t} - \frac{1}{\varepsilon^2} [j_i^n + (1 - \varepsilon^2 \eta) v \frac{D^c}{\Delta x} r_i^n] = -\frac{1}{\varepsilon^2} [j_i^{n+1} + (1 - \varepsilon^2 \eta) v \frac{D^c}{\Delta x} r_i^n].$$

168 Then,

$$169 \quad \left( \frac{1}{\Delta t} + \frac{1}{\varepsilon^2} \right) (j_i^{n+1} - j_i^n) = 0$$

170 and thus  $j_i^{n+1} = j_i^n$ .

171 The SP property of the parity equations-based AP scheme is concluded.  $\square$

172 **3. UGKS scheme for the chemotaxis kinetic model.** In this section we first extend  
 173 the UGKS in [16, 23, 24] to the time evolutionary chemotaxis model, then show its AP and SP  
 174 properties.

175 **3.1. The chemotaxis kinetic model.** The chemotaxis kinetic model models bacteria that  
 176 undergo run and tumble process as mentioned in [10, 19, 20]. During the run phase, bacteria move  
 177 along a straight line and change their directions during the tumble phase. This is called the velocity  
 178 jump process and can be modeled by the Othmer-Dunbar-Alt model that writes [2, 17]:

$$179 \quad (3.1) \quad \begin{cases} \partial_t f + \frac{1}{\varepsilon} v \cdot \nabla_x f = \frac{1}{\varepsilon^2} \left[ \frac{1}{|V|} \int_V (1 + \varepsilon \phi(v' \cdot \partial_x S)) f(v') dv' - (1 + \varepsilon \phi(v \cdot \partial_x S)) f(v) \right], \\ \partial_t S - D \Delta S + \alpha S = \beta \rho, \quad \rho(x, t) := \frac{1}{|V|} \int_V f(v) dv. \end{cases}$$

180 Here  $f(x, v, t)$  is the probability density function at time  $t$ , position  $x$  and moving with velocity  $v$ ;  
 181  $\phi$  is an odd decreasing function such that  $\phi(-u) = -\phi(u)$ ;  $S(x, t)$  is the concentration of a chemical  
 182 substance where the parameters  $D, \alpha, \beta$  are positive constants;  $\varepsilon$  is the Knudsen number. When  
 183  $\phi = 0$ , the chemotaxis kinetic model reduces to the neutron transport equation.

184 As  $\varepsilon \rightarrow 0$ ,  $f(x, v, t)$  converges to  $\rho_0(x, t)$  where  $\rho_0(x, t)$  solves the following Keller-Segel equation  
 185 [5, 11, 18]:

$$186 \quad (3.2) \quad \begin{cases} \partial_t \rho_0 = \frac{1}{3} \Delta \rho_0 + \nabla \cdot \left( \frac{1}{|V|} \int_V v \phi(v \partial_x S) dv \right) \rho_0, \\ \partial_t S - D \Delta S + \alpha S = \beta \rho_0. \end{cases}$$

187 **3.2. Discretization of the model.** Before discussing about the more complex equation for  $f$ ,  
 188 we first discretize the equation for the chemical concentration  $S$ . Let  $S_i^n \approx S(x_i, t^n)$ , the following  
 189 centered finite difference method is used to update  $S$ :

$$190 \quad (3.3) \quad \frac{S_i^{n+1} - S_i^n}{\Delta t} = D \frac{S_{i+1}^{n+1} - 2S_i^{n+1} + S_{i-1}^{n+1}}{\Delta x^2} - \alpha S_i^{n+1} + \beta \rho_i^n.$$

191 . After  $S_i^{n+1}$  are obtained, we approximate  $\partial_x S^{n+1}$  by a piecewise constant function such that

$$192 \quad (3.4) \quad \partial_x S(x, t^{n+1}) \approx \partial_x S(x_{i+\frac{1}{2}}, t^{n+1}) \approx \frac{S_{i+1}^{n+1} - S_i^{n+1}}{\Delta x} := \sigma_{i+\frac{1}{2}}, \quad \text{for } \forall x \in [x_i, x_{i+1}).$$

193 The UGKS is a finite volume approach for discretizing the kinetic equation  $f$ . By inte-  
 194 grating the chemotaxis kinetic model (3.1) over  $[x_{i-\frac{1}{2}}, x_{i+\frac{1}{2}}] \times [t^n, t^{n+1}] \times V$  and letting  $f_i^n =$   
 195  $\frac{1}{\Delta x} \int_{x_{i-\frac{1}{2}}}^{x_{i+\frac{1}{2}}} f(x, v, t^n) dx$ ,  $\rho_i^n = \frac{1}{|V|} \int_V f_i^n dv$ , the total density  $\rho_i^{n+1}$  and density fluxes  $f_i^{n+1}$  are up-  
 196 dated as follows

$$197 \quad (3.5) \quad \frac{\rho_i^{n+1} - \rho_i^n}{\Delta t} + \frac{F_{i+\frac{1}{2}}^n - F_{i-\frac{1}{2}}^n}{\Delta x} = 0,$$

$$198 \quad \frac{f_i^{n+1} - f_i^n}{\Delta t} + \frac{\Phi_{i+\frac{1}{2}}^n - \Phi_{i-\frac{1}{2}}^n}{\Delta x} = \frac{1}{\varepsilon^2} (\rho_i^{n+1} - f_i^{n+1})$$

$$199 \quad (3.6) \quad + \frac{1}{\varepsilon} \left( \frac{1}{|V|} \int_V \phi(v' \sigma_{i+\frac{1}{2}}) f_i^n(v') dv' - \phi(v \sigma_{i+\frac{1}{2}}) f_i^n \right).$$

200 Here the numerical fluxes are given by

$$201 \quad (3.7) \quad \Phi_{i+\frac{1}{2}}^n = \frac{1}{\varepsilon \Delta t} \int_{t^n}^{t^{n+1}} v f(x_{i+\frac{1}{2}}, v, t) dt,$$

$$202 \quad F_{i+\frac{1}{2}}^n = \frac{1}{|V|} \int_V \left( \frac{1}{\varepsilon \Delta t} \int_{t^n}^{t^{n+1}} v f(x_{i+\frac{1}{2}}, v, t) dt \right) dv.$$

203 It is important to note that  $\sigma_{i+\frac{1}{2}}$  approximates  $\partial_x S$  in the interval  $[x_i, x_{i+1})$  while  $f_i^n$  is the average  
 204 density over the cell  $[x_{i-\frac{1}{2}}, x_{i+\frac{1}{2}}]$ . This choice is important to get the correct advection term in the  
 205 limit Keller-Segel model when  $\varepsilon$  becomes small.

206 We use discrete ordinate method for the velocity discretization, but for convenience of explana-  
 207 tion, we write the scheme in continuous velocity. The most crucial step for UGKS is to determine  
 208  $\Phi_{i+\frac{1}{2}}^n$  and  $F_{i+\frac{1}{2}}^n$ . the details are listed below:

209 • **Find the approximation of  $f(x_{i+\frac{1}{2}}, v, t)$ .** The 1d chemotaxis model (3.1) can be  
 210 rewritten as:

$$211 \quad (3.8) \quad \partial_t f + \frac{1 + \varepsilon \phi(v \partial_x S^\varepsilon)}{\varepsilon^2} f + \frac{v}{\varepsilon} \partial_x f = \frac{1}{\varepsilon^2} \mathcal{T}^1 f,$$

212 where  $(\mathcal{T}^1 f)(x, t) := \frac{1}{|V|} \int_V (1 + \varepsilon \phi(v' \partial_x S)) f(x, v', t) dv'$ .

213 Consider the interval  $[x_i, x_{i+1})$ , multiplying both sides of (3.8) by  $\exp\left(\frac{(1 + \varepsilon \phi(v \sigma_{i+\frac{1}{2}}))}{\varepsilon^2} t\right)$   
 214 yields

$$215 \quad \frac{d}{dt} \left[ f\left(x + \frac{v}{\varepsilon} t, v, t\right) \exp\left(\frac{(1 + \varepsilon \phi(v \sigma_{i+\frac{1}{2}}))}{\varepsilon^2} t\right) \right] = \frac{\mathcal{T}^1 f(x, t)}{\varepsilon^2} \exp\left(\frac{(1 + \varepsilon \phi(v \sigma_{i+\frac{1}{2}}))}{\varepsilon^2} t\right).$$

216 Integrating the above equation over  $(t^n, t)$  yields to,

$$217 \quad (3.9) \quad \begin{aligned} f(x_{i+\frac{1}{2}}, v, t) &= f\left(x_{i+\frac{1}{2}} - \frac{v}{\varepsilon}(t - t^n), v, t^n\right) \exp\left(-\frac{(1 + \varepsilon \phi(v \sigma_{i+\frac{1}{2}}))}{\varepsilon^2}(t - t^n)\right) \\ &+ \frac{1}{\varepsilon^2} \int_{t^n}^t \mathcal{T}^1 f\left(x_{i+\frac{1}{2}} - \frac{v}{\varepsilon}(t - s), s\right) \exp\left(-\frac{(1 + \varepsilon \phi(v \sigma_{i+\frac{1}{2}}))}{\varepsilon^2}(t - s)\right) ds. \end{aligned}$$

218 This is an exact expression for  $f(x_{i+\frac{1}{2}}, v, t)$  that will be used to determine  $\Phi_{i+\frac{1}{2}}^n, F_{i+\frac{1}{2}}^n$  in  
 219 (3.7). At this stage, we need to approximate  $f(x, v, t^n)$  and  $(\mathcal{T}^1 f)(x, t)$  on the right hand  
 220 side of (3.9).  $f$  is approximated by a piecewise constant function and  $\mathcal{T}^1 f$  by a piecewise  
 221 linear function as follows:

$$222 \quad \begin{aligned} f(x, v, t^n) &= \begin{cases} f_i^n, & x < x_{i+\frac{1}{2}}, \\ f_{i+1}^n, & x > x_{i+\frac{1}{2}}, \end{cases} \\ \mathcal{T}^1 f(x, t) &= \begin{cases} \mathcal{T}^1 f_{i+\frac{1}{2}}^n + \delta^L \mathcal{T}^1 f_{i+\frac{1}{2}}^n (x - x_{i+\frac{1}{2}}), & x < x_{i+\frac{1}{2}}, \\ \mathcal{T}^1 f_{i+\frac{1}{2}}^n + \delta^R \mathcal{T}^1 f_{i+\frac{1}{2}}^n (x - x_{i+\frac{1}{2}}), & x > x_{i+\frac{1}{2}}. \end{cases} \end{aligned}$$

223 Here  $\mathcal{T}^1 f_{i+\frac{1}{2}}^n, \delta^L \mathcal{T}^1 f_{i+\frac{1}{2}}^n, \delta^R \mathcal{T}^1 f_{i+\frac{1}{2}}^n$  are defined by:

$$224 \quad \begin{cases} \mathcal{T}^1 f_{i+\frac{1}{2}}^n := \frac{1}{|V^-|} \int_{V^-} (1 + \varepsilon \phi(v \sigma_{i+\frac{1}{2}})) f_{i+1}^n + \frac{1}{|V^+|} \int_{V^+} (1 + \varepsilon \phi(v \sigma_{i+\frac{1}{2}})) f_i^n, \\ \delta^L \mathcal{T}^1 f_{i+\frac{1}{2}}^n := \frac{\mathcal{T}^1 f_{i+\frac{1}{2}}^n - \mathcal{T}^1 f_i^n}{\Delta x/2}, \\ \delta^R \mathcal{T}^1 f_{i+\frac{1}{2}}^n := \frac{\mathcal{T}^1 f_{i+1}^n - \mathcal{T}^1 f_{i+\frac{1}{2}}^n}{\Delta x/2}, \end{cases}$$

225 with  $V^+ = V \cap \mathbb{R}^+$  and  $V^- = V \cap \mathbb{R}^-$ .

226 Substituting the above approximations into (3.9) yields an expression for  $f(x_{i+\frac{1}{2}}, v, t)$  such



227 that:  
228 For  $v > 0$ ,

$$\begin{aligned}
 f(x_{i+\frac{1}{2}}, v, t) &= f_i^n \exp\left(-\frac{(1 + \varepsilon\phi(v\sigma_{i+\frac{1}{2}}))}{\varepsilon^2}(t - t^n)\right) + \frac{\mathcal{T}^1 f_{i+\frac{1}{2}}^n}{1 + \varepsilon\phi(v\sigma_{i+\frac{1}{2}})} \\
 (3.10) \quad &\times \left(1 - \exp\left(-\frac{(1 + \varepsilon\phi(v\sigma_{i+\frac{1}{2}}))}{\varepsilon^2}(t - t^n)\right)\right) + v\varepsilon \frac{\delta^L \mathcal{T}^1 f_{i+\frac{1}{2}}^n}{(1 + \varepsilon\phi(v\sigma_{i+\frac{1}{2}}))^2} \\
 &\times \left[\left(1 + \frac{1 + \varepsilon\phi(v\sigma_{i+\frac{1}{2}})}{\varepsilon^2}(t - t^n)\right) \exp\left(-\frac{(1 + \varepsilon\phi(v\sigma_{i+\frac{1}{2}}))}{\varepsilon^2}(t - t^n)\right) - 1\right],
 \end{aligned}$$

230 and for  $v < 0$ ,

$$\begin{aligned}
 f(x_{i+\frac{1}{2}}, v, t) &= f_{i+1}^n \exp\left(-\frac{(1 + \varepsilon\phi(v\sigma_{i+\frac{1}{2}}))}{\varepsilon^2}(t - t^n)\right) + \frac{\mathcal{T}^1 f_{i+\frac{1}{2}}^n}{1 + \varepsilon\phi(v\sigma_{i+\frac{1}{2}})} \\
 (3.11) \quad &\times \left(1 - \exp\left(-\frac{(1 + \varepsilon\phi(v\sigma_{i+\frac{1}{2}}))}{\varepsilon^2}(t - t^n)\right)\right) + v\varepsilon \frac{\delta^R \mathcal{T}^1 f_{i+\frac{1}{2}}^n}{(1 + \varepsilon\phi(v\sigma_{i+\frac{1}{2}}))^2} \\
 &\times \left[\left(1 + \frac{1 + \varepsilon\phi(v\sigma_{i+\frac{1}{2}})}{\varepsilon^2}(t - t^n)\right) \exp\left(-\frac{(1 + \varepsilon\phi(v\sigma_{i+\frac{1}{2}}))}{\varepsilon^2}(t - t^n)\right) - 1\right].
 \end{aligned}$$

232 • **Determine**  $\Phi_{i+\frac{1}{2}}^n, F_{i+\frac{1}{2}}^n$ . The flux  $\Phi_{i+\frac{1}{2}}^n(v)$  in (3.7) can be approximated by

$$\begin{aligned}
 (3.12) \quad \Phi_{i+\frac{1}{2}}^n(v) &= Avf_{i+1}^n + Bv\mathcal{T}^1 f_{i+\frac{1}{2}}^n + Cv^2\delta^R\mathcal{T}^1 f_{i+\frac{1}{2}}^n, \quad \text{for } v < 0, \\
 \Phi_{i+\frac{1}{2}}^n(v) &= Avf_i^n + Bv\mathcal{T}^1 f_{i+\frac{1}{2}}^n + Cv^2\delta^L\mathcal{T}^1 f_{i+\frac{1}{2}}^n, \quad \text{for } v > 0,
 \end{aligned}$$

234 where the coefficients  $A(v, \varepsilon, \Delta t), B(v, \varepsilon, \Delta t), C(v, \varepsilon, \Delta t)$  can be determined explicitly such  
235 that

$$\begin{aligned}
 A(v, \varepsilon, \Delta t) &:= \frac{\varepsilon}{\Delta t(1 + \varepsilon\phi(v\sigma_{i+\frac{1}{2}}))} \left(1 - \exp\left(-\frac{1 + \varepsilon\phi(v\sigma_{i+\frac{1}{2}})}{\varepsilon^2}\Delta t\right)\right), \\
 B(v, \varepsilon, \Delta t) &:= \frac{1}{\varepsilon(1 + \varepsilon\phi(v\sigma_{i+\frac{1}{2}}))} \\
 (3.13) \quad &- \frac{\varepsilon}{\Delta t(1 + \varepsilon\phi(v\sigma_{i+\frac{1}{2}}))^2} \left(1 - \exp\left(-\frac{1 + \varepsilon\phi(v\sigma_{i+\frac{1}{2}})}{\varepsilon^2}\Delta t\right)\right), \\
 C(v, \varepsilon, \Delta t) &:= \frac{2\varepsilon^2}{\Delta t(1 + \varepsilon\phi(v\sigma_{i+\frac{1}{2}}))^3} \left(1 - \exp\left(-\frac{1 + \varepsilon\phi(v\sigma_{i+\frac{1}{2}})}{\varepsilon^2}\Delta t\right)\right) \\
 &- \frac{1}{(1 + \varepsilon\phi(v\sigma_{i+\frac{1}{2}}))^2} \left(1 + \exp\left(-\frac{1 + \varepsilon\phi(v\sigma_{i+\frac{1}{2}})}{\varepsilon^2}\Delta t\right)\right).
 \end{aligned}$$

237 Furthermore,  $F_{i+\frac{1}{2}}^n$  in (3.7) is given by

(3.14)

$$\begin{aligned}
F_{i+\frac{1}{2}}^n &= \frac{1}{|V|} \int_{V^-} Av f_{i+1}^n dv + \frac{1}{|V|} \int_{V^+} Av f_i^n dv + \frac{1}{|V|} \mathcal{T}^1 f_{i+\frac{1}{2}}^n \int_V v B dv \\
&\quad + \frac{1}{|V|} \delta^R \mathcal{T}^1 f_{i+\frac{1}{2}}^n \int_{V^-} C v^2 dv + \frac{1}{|V|} \delta^L \mathcal{T}^1 f_{i+\frac{1}{2}}^n \int_{V^+} C v^2 dv.
\end{aligned}$$

This concludes the construction of the scheme. For the proof of its AP property, one can refer to Appendix A.

**3.3. SP Property.** Assume that we start from a steady state solution that at the discrete level satisfies,

$$(3.15) \quad \frac{\Phi_{i+\frac{1}{2}}^n - \Phi_{i-\frac{1}{2}}^n}{\Delta x} = \frac{1}{\varepsilon^2} (\rho_i^n - f_i^n) + \frac{1}{\varepsilon} \left( \frac{1}{|V|} \int_V \phi(v' \sigma_{i+\frac{1}{2}}) f_i^n(v') dv' - \phi(v \sigma_{i+\frac{1}{2}}) f_i^n \right).$$

Integrating (3.15) over  $v$  yields

$$\frac{F_{i+\frac{1}{2}}^n - F_{i-\frac{1}{2}}^n}{\Delta x} = 0,$$

From (3.5) one can deduce that,

$$(3.16) \quad \rho_i^{n+1} = \rho_i^n,$$

which indicates that the macroscopic density is preserved. Using (3.15), the equation of updating  $f^{n+1}$  in (3.6) can be written as,

$$\frac{f_i^{n+1} - f_i^n}{\Delta t} = \frac{1}{\varepsilon^2} \left( (\rho_i^{n+1} - \rho_i^n) - (f_i^{n+1} - f_i^n) \right).$$

Then from (3.16),

$$\left( 1 + \frac{\Delta t}{\varepsilon^2} \right) (f_i^{n+1} - f_i^n) = 0,$$

which gives  $f_i^{n+1} = f_i^n$ . This concludes the SP property of the UGKS.

**4. IMEX scheme with the Penalization method for the Boltzmann equation.** In this section, we consider the penalization method developed in [8] for the Boltzmann equation. This method together with an IMEX discretization of the equation give an AP scheme for the Boltzmann equation. One can find the AP proof in [8]. Here we show that the penalization method is not only AP but also SP as well.

**4.1. The Boltzmann equation.** The Boltzmann equation describes the time evolution of the density distribution of gas particles. It is given by

$$\partial_t f + v \nabla_x f = \frac{\mathcal{Q}(f)}{\varepsilon}.$$

Here  $f(x, v, t)$  is the probability density distribution of particles at time  $t$ , position  $x$  and with velocity  $v$ .  $\mathcal{Q}$  is the Boltzmann collision operator where only binary interactions are considered.

268 Let  $(v, v_*)$  and  $(v', v'_*)$  be respectively the velocities of the two colliding particles before and after  
 269 the collision related by

$$270 \quad \begin{cases} v' = \frac{1}{2}((v - v_*) - |v - v_*|\sigma), \\ v'_* = \frac{1}{2}((v - v_*) + |v - v_*|\sigma). \end{cases}$$

271 with  $\sigma \in \mathcal{S}^{d_v-1}$ .  $\mathcal{Q}$  is given by

$$272 \quad \mathcal{Q}(f)(v) = \int_{\mathbb{R}^{d_v}} \int_{\mathbb{S}^{d_v-1}} B(|v - v_*|, \cos \theta)(f(v'_*)f(v') - f(v_*)f(v))d\sigma dv_*.$$

273 The collision kernel  $B$  is a non-negative function given by  $B(|u|, \cos \theta) = C_\alpha |u|^\alpha$  where  $u = \frac{(v - v_*)}{|v - v_*|}$   
 274 and  $\cos \theta = u \cdot \sigma$ . For more details, one can look at the Boltzmann equation description in [8].  $\varepsilon$  is  
 275 the dimensionless Knudsen number and  $\int_v \alpha(v) \mathcal{Q}(f) dv = 0$  for  $\alpha(v) = (1, v, |v|^2)$ . The equilibrium  
 276 distribution of  $\mathcal{Q}$  is the Maxwellian distribution  $\mathcal{M}_{\rho, u, T}$ , i.e.  $\mathcal{Q}(\mathcal{M}_{\rho, u, T}) = 0$ . As  $\varepsilon \rightarrow 0$ , the  
 277 moments of the distribution function solve the Euler equations (1.2).

278 **4.2. IMEX scheme with the Penalization method.** The penalization method was origi-  
 279 nally developed in [8, 21]. The idea is to split the collision term of the Boltzmann equation into  
 280 a stiff part and less stiff part. More precisely, the Boltzmann equation is written in the following  
 281 form:

$$282 \quad \partial_t f + v \nabla_x f = \frac{\mathcal{Q}(f) - P(f)}{\varepsilon} + \frac{P(f)}{\varepsilon},$$

284 where  $\mathcal{Q}(f)$  is the Boltzmann collision operator and  $P(f)$  is a relaxation operator, namely  $P(f) =$   
 285  $\beta[\mathcal{M}_{\rho, u, T}(v) - f(v)]$  where  $\beta$  is a strictly positive parameter.  $P(f)$  has the same equilibrium as  
 286  $\mathcal{Q}(f)$ . It satisfies  $\int_v P(f) \alpha(v) dv = 0$  for  $\alpha(v) = (1, v, |v|^2)$  and  $P(\mathcal{M}_{\rho, u, T}) = 0$ . As in [8],  $\beta^n$  is  
 287 chosen to be  $2\pi\rho^n$  such that both operators  $P(f)$  and the full Boltzmann operator  $\mathcal{Q}(f)$  have the  
 288 same loss term corresponding to the dissipative part.

289 The following IMEX discretization of the Boltzmann equation is proposed in [8]:

$$290 \quad (4.1) \quad \frac{f^{n+1} - f^n}{\Delta t} + v \cdot \nabla_x f^n = \frac{\mathcal{Q}(f^n) - P(f^n)}{\varepsilon} + \frac{P(f^{n+1})}{\varepsilon}.$$

291 For the discretization of the Boltzmann operator one can use a fast spectral Fourier-Galerkin  
 292 method [7], and for the transport part, a first or second order finite volume scheme can be employed.  
 293 This gives an AP discretization for the Boltzmann equation as proved in [8].

294 **4.3. SP property.** Suppose that the solution satisfies the stationary equation at time  $t^n$ , i.e.

$$295 \quad (4.2) \quad v \cdot \nabla_x f^n = \frac{\mathcal{Q}(f^n) - P(f^n)}{\varepsilon} + \frac{P(f^n)}{\varepsilon}.$$

296 It follows from the properties of the collision operator  $\mathcal{Q}$  and the relaxation operator  $P$  that:

$$297 \quad (4.3) \quad \int_v \alpha(v) v \cdot \nabla_x f^n = 0,$$

298 with  $\alpha(v) = (1, v, |v|^2)$ .

299 Now multiply (4.1) by  $\alpha(v)$  and integrate over the velocity space. Using the conservation properties

300 of  $\mathcal{Q}$ ,  $P$  and (4.3), one gets that the macroscopic quantities are preserved. Then  $\mathcal{M}^{n+1} = \mathcal{M}^n$  and  
 301  $\beta^{n+1} = \beta^n$ . By adding and subtracting  $\beta^n f^n / \varepsilon$ , Eq.(4.1) can be written as:

$$302 \quad \frac{f^{n+1} - f^n}{\Delta t} + v \cdot \nabla_x f^n = \frac{\mathcal{Q}(f^n) - P(f^n)}{\varepsilon} + \frac{\beta^n [\mathcal{M}^n - f^n]}{\varepsilon} - \frac{\beta^n [f^{n+1} - f^n]}{\varepsilon}.$$

303 Noting that  $f^n$  satisfies the steady state equation (4.2), one gets

$$304 \quad \frac{f^{n+1} - f^n}{\Delta t} + \frac{\beta^n [f^{n+1} - f^n]}{\varepsilon} = 0,$$

305 Thus  $f^{n+1} = f^n$ . The steady state is preserved.

306 **5. Experimental results.** Three test cases are considered in this section, each validates the  
 307 AP and SP properties of one scheme presented in section 2, 3 or 4.

308 **5.1. Neutron transport equation-Parity equations-based scheme.** To validate the AP  
 309 and SP properties of the parity equations-based scheme, we use the same initial and boundary  
 310 conditions as problem 1 in section 6 in [22]. The initial distribution is  $f(x, v, t = 0) = 0$  and the  
 311 computational domain is  $x \in [0, 1]$ . The boundary conditions are as in (2.8) and (2.9) with

$$312 \quad F_L(v) = 1 \text{ and } F_R(v) = 0.$$

313 This data is consistent as can be seen by (2.8) and (2.9). The mesh and time step sizes are  
 314 respectively  $\Delta x = 0.025$  and  $\Delta t = 0.0002$ . In Figure 1, we plot the density at time  $t = 0.05$  for  
 315  $\varepsilon = 10^{-2}$ ,  $\varepsilon = 10^{-3}$ ,  $\varepsilon = 10^{-6}$  and compare it to its diffusion limit. The curves get close to each  
 316 other when  $\varepsilon$  gets very small. The curve corresponding to  $\varepsilon = 10^{-6}$  is exactly on top of the curve  
 317 of the diffusion limit equation. This verifies the AP property. Furthermore, we plot in Figure 2  
 318 the time evolution of the distance between the numerical stationary solution  $\rho_r^s$  and the numerical  
 319 solution  $\rho_r$  of the time evolutionary equation given by the  $L^\infty$  norm

$$320 \quad \|\rho_r - \rho_r^s\|_\infty = \max_j \{\rho_{rj} - \rho_{rj}^s\}.$$

321 One can see that this distance does not change after we reach the steady state at  $t = 10$ . After that  
 322 we give the norm at discrete times in Table 2 where we also show that the SP property is valid for  
 323 all  $\varepsilon \ll 1$ . Figure 2 and Table 2 indicate that the SP property is well satisfied.

$\varepsilon = 10^{-3}$	Time	0	2	4	10	20
	$L_\infty$ -norm	1	$9.730 \times 10^{-4}$	$5.042 \times 10^{-4}$	$5.042 \times 10^{-4}$	$5.042 \times 10^{-4}$
$\varepsilon = 10^{-8}$	Time	0	4	8	10	20
	$L_\infty$ -norm	1	$1.263 \times 10^{-6}$	$1.053 \times 10^{-12}$	$1.269 \times 10^{-12}$	$1.269 \times 10^{-12}$

TABLE 2

Neutron Transport:  $L_\infty$ -norm of the difference between the solution and the stationary solution in the time interval  $[0, 20]$  for different  $\varepsilon$ .

324 **5.2. Chemotaxis kinetic model-UGKS scheme.** Parameters in (3.1) are chosen as in [9]  
 325 such that,

$$326 \quad \chi_S = 1, D = 15, \beta = 60, \alpha = 3.$$

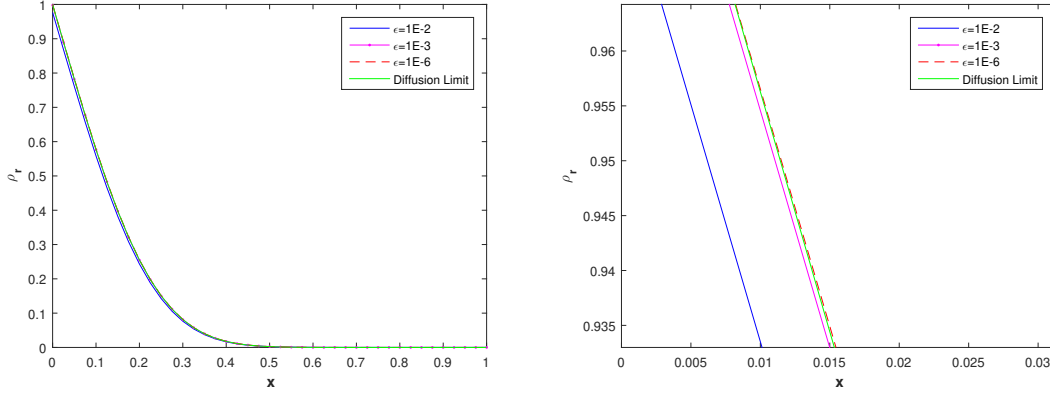


FIG. 1. Verification of the AP property of the parity equations-based scheme for the neutron Transport equation. Left: The density  $\rho_r$  at time  $t = 0.05$  for  $\epsilon = 10^{-2}$ ,  $\epsilon = 10^{-3}$ ,  $\epsilon = 10^{-6}$  and the solution of the diffusion limit equation; right: a zoomed part of the left plot.

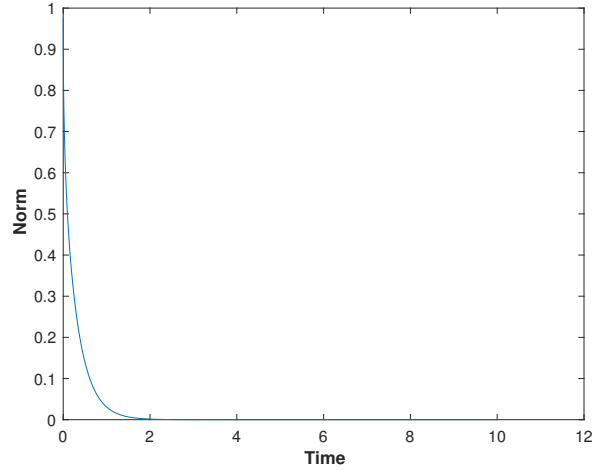


FIG. 2. Neutron Transport: Time evolution of the  $L_\infty$ -norm of the difference between the solution (starting from initial data  $f = 0$ ) and the stationary solution (starting from the steady  $f$  at time  $t = 10$ ) in the time interval  $[0, 10]$  for  $\epsilon = 10^{-8}$ .

327 and  $\phi$  is of the form

328 
$$\phi(u) = -\chi_S \tanh u.$$

329 The computational domain is set to be  $x \in [-1, 1]$ . We impose specular boundary conditions for  $f$   
 330 and Dirichlet conditions for  $S$ . The initial density distribution is composed of two bumps located

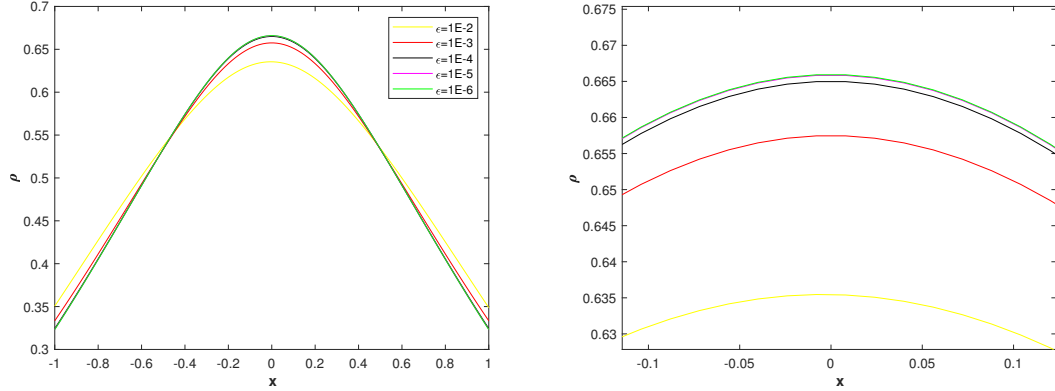


FIG. 3. Verification of the AP property of the UGKS for the chemotaxis kinetic model. Left: The density  $\rho$  at time  $t = 1$  for  $\varepsilon = 10^{-2}, 10^{-3}, 10^{-4}, 10^{-5}, 10^{-6}$ ; right: a zoomed part of the left plot.

331 at  $x = \pm 0.65$  given by:

$$332 \quad f(x, v, 0) = 5(\exp(-10(x - 0.65)^2 - 20(v + 0.45)^2) + \exp(-10(x + 0.65)^2 - 20(v - 0.45)^2)).$$

333 We use  $\Delta x = 2/500$  for the space discretization and  $v \in [-1, 1]$  with the  $S_{32}$  Gaussian quadrature  
 334 points for the velocity. The limiting scheme of the UGKS is an explicit solver for the diffusion  
 335 equation. Therefore, to ensure the stability of the numerical scheme, the time step  $\Delta t$  is chosen as  
 336 below

$$337 \quad \Delta t = \begin{cases} 0.5\Delta x^2, & \text{for } \varepsilon < \Delta x, \\ 0.5\varepsilon\Delta x, & \text{else.} \end{cases}$$

338 In order to verify the AP property of our scheme, the total densities  $\rho$  at time  $t = 1$  are displayed  
 339 in Figure 3 for different values of  $\varepsilon$  ranging from  $10^{-2}$  to  $10^{-6}$ . In order to check the SP property,  
 340 we ran our simulations till it reaches a steady state then we consider this as our initial data. Time  
 341 evolution of the  $L_\infty$ -norm of the difference between the solution (starting from initial data) and  
 342 the stationary solution in the time interval  $[0, 100]$  is displayed in Table 3 for  $\varepsilon = 1$  and  $\varepsilon = 10^{-3}$ .  
 These results ensure that the SP property is independent of  $\varepsilon$ .

$\varepsilon = 1$	Time	0	30	60	65	100
	$L_\infty$ -norm	0.9064	$8.192 \times 10^{-7}$	$3.737 \times 10^{-11}$	$7.385 \times 10^{-12}$	$1.573 \times 10^{-12}$
$\varepsilon = 10^{-3}$	Time	0	5	10	50	100
	$L_\infty$ -norm	0.6493	$2.968 \times 10^{-7}$	$9.999 \times 10^{-10}$	$1.476 \times 10^{-10}$	$1.476 \times 10^{-10}$

TABLE 3

Chemotaxis:  $L_\infty$ -norm of the difference between the solution and the stationary solution in the time interval  $[0, 100]$  for different  $\varepsilon$ .

343

344 **5.3. The Boltzmann equation-IMEX scheme with the Penalization method .** In this  
 345 section we consider the 2D Bose gas experiment 3.3 in [12] to test the AP and the SP property of

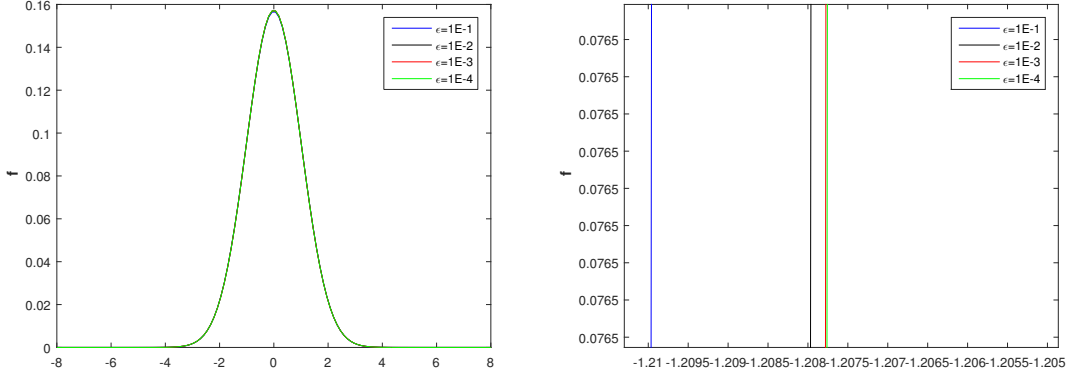


FIG. 4. Boltzmann: cross section of the distribution function for different values of  $\varepsilon$ (left) and a zoomed part of the plot(right).

346 the penalization method presented in [8]. We solve the space homogeneous quantum Boltzmann  
 347 equation in 2D velocity space which is a special case of the classical Boltzmann equation for a  
 348 particular collision operator  $\mathcal{Q}_q$ (the quantum collision operator) [12].

$$349 \quad \partial_t f = \frac{\mathcal{Q}_q(f) - P(f)}{\varepsilon} + \frac{P(f)}{\varepsilon}. \quad 350$$

351 The idea can be extended to more general collision operators. Hence, scheme (4.1) is simplified to

$$352 \quad f^{n+1} = \frac{\varepsilon}{\varepsilon + \beta^{n+1}\Delta t} f^n + \Delta t \frac{\mathcal{Q}_q(f^n) - P(f^n)}{\varepsilon + \beta^{n+1}\Delta t} + \frac{\beta^{n+1}\Delta t}{\varepsilon + \beta^{n+1}\Delta t} \mathcal{M}^{n+1}.$$

353 The initial distribution function is given as in [12],

$$354 \quad f_0(v) = \frac{\rho_0}{4\pi T_0} \left( \exp\left(\frac{-|v - u_0|^2}{2T_0}\right) + \exp\left(\frac{-|v + u_0|^2}{2T_0}\right) \right),$$

355 where  $\rho_0 = 1$ ,  $T_0 = 3/8$ , and  $u_0 = (1, 1/2)$ . The computational domain is  $[-8, 8]^2$  with 64 grid  
 356 points. The quantum Maxwellian [12] is given as,

$$357 \quad M_q(v) = \frac{1}{\theta_0} \frac{1}{z^{-1} \exp\left(\frac{(v-u)^2}{2T}\right) - 1}.$$

358 where  $\theta_0 = 0.1^2$ ,  $z = 0.001590$ ,  $T = 1$  is the temperature and  $u = 0$  is the macroscopic velocity. In  
 359 Figure 4 we test the AP property of the penalization method. A cross section of the distribution  
 360 function for different values of  $\varepsilon$  is plotted on the left and a zoomed part of the plot on the  
 361 right. The curves are getting closer to each other as  $\varepsilon$  converges to 0 which implies that the AP  
 362 property is satisfied. Moreover, we investigate the SP property. Figure 5 is a comparison between  
 363 the distribution function at the final time  $t = 100$  and the Maxwellian distribution. We run our  
 364 simulation till  $t = 100$  where the equilibrium is reached and then use this equilibrium as new initial

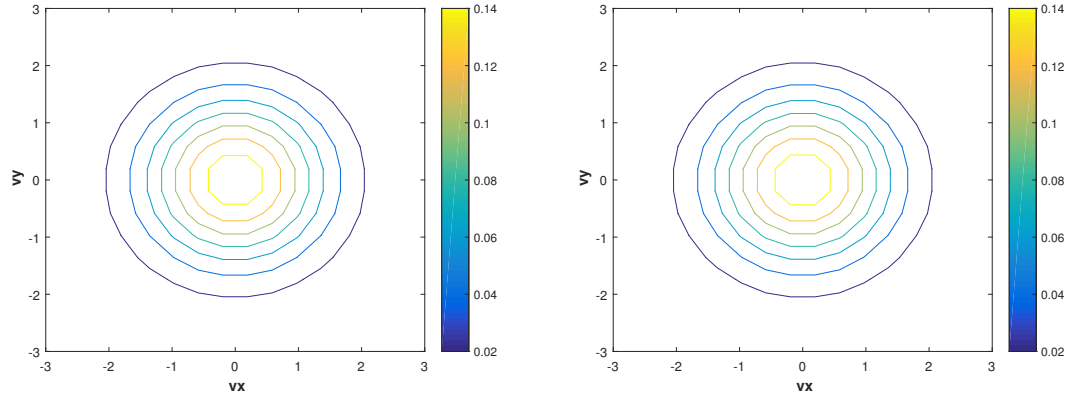


FIG. 5. Boltzmann: contours of the 2D distribution function at the final time  $t = 100$  (left) and the Maxwellian distribution function (right).

365 data till  $t = 100$ . We computed the  $L_\infty$ -norm of the difference between  $f$  and its equilibrium in the  
 366 time interval  $[0, 100]$  in Figure 6 as an evidence that  $f$  converges exponentially to the equilibrium.  
 367 Table 4 presents the discrete times where one can find exactly when the initial distribution function  
 368 reaches its equilibrium.

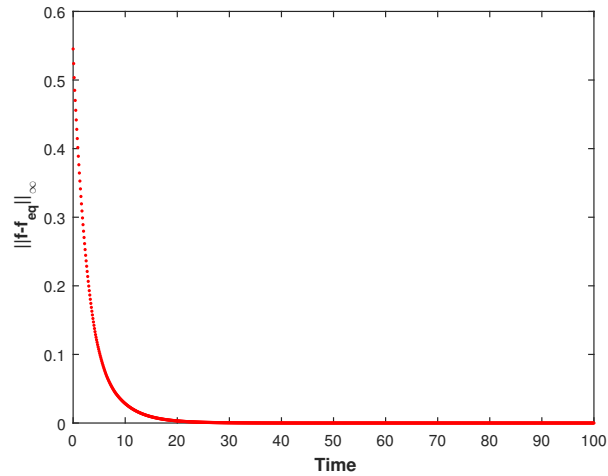


FIG. 6. Boltzmann: Time evolution of the  $L_\infty$ -norm of the difference between the distribution function  $f$  and its equilibrium in the time interval  $[0, 100]$ .

369 **6. Conclusion.** In this work we find out that these three AP schemes have something in  
 370 common. In the three schemes, once one is able to show that the macroscopic quantities can be  
 371 updated explicitly then we are able to prove that scheme is SP. Whether this is true in general or



Time	0	20	60	85	90	100
$L_\infty$ -norm	0.5453	$3.1 \times 10^{-3}$	$1.393 \times 10^{-5}$	$1.464 \times 10^{-5}$	$1.464 \times 10^{-5}$	$1.464 \times 10^{-5}$

TABLE 4

Boltzmann:  $L_\infty$ -norm of the difference between  $f$  and its equilibrium starting from  $t=0$  till the final time  $t=100$  for  $\varepsilon = 1$ .

not remains a future work.

**Appendix A. AP property of the UGKS.** In this part, we give a formal derivation of the AP property for the UGKS proposed in (3.5)–(3.6).

When  $\varepsilon$  goes to zero, asymptotic expansions of  $A, B, C$  given in (3.13) read  $A = O(\varepsilon)$ ,  $B = \frac{1}{\varepsilon} - \phi(v\sigma_{i+\frac{1}{2}}) + O(\varepsilon)$ ,  $C = -1 + O(\varepsilon)$ . The leading order term of (3.6) yields  $f_i^{n+1} = \rho_i^{n+1} + O(\varepsilon)$  and we only need to show that (3.5) satisfies the equation for  $\rho$  in (3.2), at the discrete level. Suppose that  $f_i^n = \rho_i^n + O(\varepsilon)$ , then

$$\begin{cases} \mathcal{T}^1 f_{i+\frac{1}{2}}^n = \frac{1}{2} (\rho_i^n + \rho_{i+1}^n) + O(\varepsilon), \\ \delta^L \mathcal{T}^1 f_{i+\frac{1}{2}}^n = \frac{\rho_{i+1}^n - \rho_i^n}{\Delta x} + O(\varepsilon), \\ \delta^R \mathcal{T}^1 f_{i+\frac{1}{2}}^n = \frac{\rho_{i+1}^n - \rho_i^n}{\Delta x} + O(\varepsilon). \end{cases}$$

We deduce that the expansion of  $F_{i+\frac{1}{2}}^n$  reads:

$$F_{i+\frac{1}{2}}^n = -\frac{\rho_i^n + \rho_{i+1}^n}{2|V|} \left( \int_V v \phi(v\sigma_{i+\frac{1}{2}}) dv \right) - \frac{\rho_{i+1}^n - \rho_i^n}{3\Delta x} + O(\varepsilon).$$

Therefore,

$$(A.1) \quad \frac{F_{i+\frac{1}{2}}^n - F_{i-\frac{1}{2}}^n}{\Delta x}$$

$$(A.2) \quad = -\frac{\rho_{i+1}^n - 2\rho_i^n + \rho_{i-1}^n}{3(\Delta x)^2} + \left( -\left( \frac{1}{|V|} \int_V v \phi(v\sigma_{i+\frac{1}{2}}) dv \right) \frac{\rho_i^n + \rho_{i+1}^n}{2} \right.$$

$$(A.3) \quad \left. + \left( \frac{1}{|V|} \int_V v \phi(v\sigma_{i-\frac{1}{2}}) dv \right) \frac{\rho_i^n + \rho_{i-1}^n}{2} \right) + O(\varepsilon).$$

In the limit of  $\varepsilon \rightarrow 0$ , the discretization (3.5) becomes

$$\begin{aligned} \frac{\rho_i^{n+1} - \rho_i^n}{\Delta t} &= \frac{\rho_{i+1}^n - 2\rho_i^n + \rho_{i-1}^n}{3(\Delta x)^2} \\ &+ \left( \frac{1}{|V|} \left( \int_V v \phi(v\sigma_{i+\frac{1}{2}}) dv \right) \frac{\rho_i^n + \rho_{i+1}^n}{2} - \frac{1}{|V|} \left( \int_V v \phi(v\sigma_{i-\frac{1}{2}}) dv \right) \frac{\rho_i^n + \rho_{i-1}^n}{2} \right). \end{aligned}$$

which is a consistent discretization of the equation for  $\rho$  in (3.2). Therefore, the proposed scheme is AP after coupling with the discretization for  $S(x, t)$  in (3.3).

REFERENCES

REFERENCES

- 394 [1] M. ADAMS, *Discontinuous finite element transport solutions in thick diffusive problems*, Nuclear Science and  
 395 Engineering, 137 (2001), pp. 298–333, <https://doi.org/http://dx.doi.org/10.13182/NSE00-41>.
- 396 [2] W. ALT, *Biased random walk models for chemotaxis and related diffusion approximations*, Journal of Mathe-  
 397 matical Biology, 9 (1980), pp. 147–177, <https://doi.org/10.1007/BF00275919>, <http://dx.doi.org/10.1007/>  
 398 [BF00275919](http://dx.doi.org/10.1007/BF00275919).
- 399 [3] J. A. CARRILLO AND B. YAN, *An asymptotic preserving scheme for the diffusive limit of kinetic systems*  
 400 *for chemotaxis*, Multiscale Model. Simul., 11 (2013), pp. 336–361, <https://doi.org/10.1137/110851687>,  
 401 <http://dx.doi.org/10.1137/110851687>.
- 402 [4] C. CERCIGNANI, *The Boltzmann equation and its applications*, Springer, 1988.
- 403 [5] F. CHALUB, P. MARKOWICH, B. PERTHAME, AND C. SCHMEISER, *Kinetic models for chemotaxis and their drift-*  
 404 *diffusion limits*, Monatsh. Math., 142 (2004), pp. 123–141, <https://doi.org/10.1007/s00605-004-0234-7>,  
 405 <http://dx.doi.org/10.1007/s00605-004-0234-7>.
- 406 [6] K. A. M. M. O. S. CHERTOCK, A., *An asymptotic preserving scheme for kinetic chemotaxis models in two*  
 407 *space dimensions*, submitted, (2017).
- 408 [7] F.FILBET, C.MOUHOT, AND L.PARESCHI, *Solving the boltzmann equation in  $n \log_2 n$* , SIAM Journal of scientific  
 409 computation, 28 (2006), pp. 1029–1053.
- 410 [8] F. FILBET AND S. JIN, *A class of asymptotic-preserving schemes for kinetic equations and related problems*  
 411 *with stiff sources*, Journal of Computational Physics, 229 (2010), pp. 7625–7648, [https://doi.org/10.1016/](https://doi.org/10.1016/j.jcp.2010.06.017)  
 412 <http://www.sciencedirect.com/science/article/pii/S0021999110003323>.
- 413 [9] L. GOSSE, *A well-balanced scheme for kinetic models of chemotaxis derived from one-dimensional local forward-*  
 414 *backward problems*, Math. Biosci., 242 (2013), pp. 117–128, <https://doi.org/10.1016/j.mbs.2012.12.009>,  
 415 <http://dx.doi.org/10.1016/j.mbs.2012.12.009>.
- 416 [10] B. HOWARD, *E. coli in Motion*, Biological and Medical Physics, Biomedical Engineering, Springer, 2004.
- 417 [11] H. J. HWANG, K. KANG, AND A. STEVENS, *Drift-diffusion limits of kinetic models for chemotaxis: a generaliza-*  
 418 *tion*, Discrete Contin. Dyn. Syst. Ser. B, 5 (2005), pp. 319–334, <https://doi.org/10.3934/dcdsb.2005.5.319>,  
 419 <http://dx.doi.org/10.3934/dcdsb.2005.5.319>.
- 420 [12] J.HU AND L.YING, *A fast spectral algorithm for the quantum boltzmann collision operator*, COMMUN. MATH.  
 421 SCI., 10 (2012), pp. 989–999.
- 422 [13] S. JIN, M. TANG, AND H. HAN, *A uniformly second order numerical method for the one-dimensional discrete-*  
 423 *ordinate transport equation and its diffusion limit with interface*, Netw. Heterog. Media, 4 (2009), pp. 35–65,  
 424 <https://doi.org/10.3934/nhm.2009.4.35>, <http://dx.doi.org/10.3934/nhm.2009.4.35>.
- 425 [14] E. W. LARSEN, J. MOREL, AND W. F. M. JR, *Asymptotic solutions of numerical transport problems*  
 426 *in optically thick, diffusive regimes*, Journal of Computational Physics, 69 (1987), pp. 283 – 324,  
 427 [https://doi.org/http://dx.doi.org/10.1016/0021-9991\(87\)90170-7](https://doi.org/http://dx.doi.org/10.1016/0021-9991(87)90170-7), <http://www.sciencedirect.com/science/>  
 428 [article/pii/0021999187901707](http://www.sciencedirect.com/science/article/pii/0021999187901707).
- 429 [15] E. W. LARSEN AND J. E. MOREL, *Asymptotic solutions of numerical transport problems in optically*  
 430 *thick, diffusive regimes ii*, J. Comput. Phys., 69 (1989), pp. 212–236.
- 431 [16] L. MIEUSSENS, *On the asymptotic preserving property of the unified gas kinetic scheme for the diffusion limit*  
 432 *of linear kinetic models*, J. Comput. Phys., 253 (2013), pp. 138–156, [https://doi.org/10.1016/j.jcp.2013.](https://doi.org/10.1016/j.jcp.2013.07.002)  
 433 [07.002](http://dx.doi.org/10.1016/j.jcp.2013.07.002), <http://dx.doi.org/10.1016/j.jcp.2013.07.002>.
- 434 [17] H. OTHMER, S. DUNBAR, AND W. ALT, *Models of dispersal in biological systems*, J. Math. Biol., 26 (1988),  
 435 pp. 263–298, <https://doi.org/10.1007/BF00277392>, <http://dx.doi.org/10.1007/BF00277392>.
- 436 [18] H. OTHMER AND T. HILLEN, *The diffusion limit of transport equations. II. Chemotaxis equations*, SIAM J.  
 437 Appl. Math., 62 (2002), pp. 1222–1250 (electronic), <https://doi.org/10.1137/S0036139900382772>, [http://](http://dx.doi.org/10.1137/S0036139900382772)  
 438 [dx.doi.org/10.1137/S0036139900382772](http://dx.doi.org/10.1137/S0036139900382772).
- 439 [19] J. SARAGOSTI, V. CALVEZ, N. BOURNAVEAS, A. BUGUIN, P. SILBERZAN, AND B. PERTHAME, *Mathematical*  
 440 *description of bacterial traveling pulses*, PLoS Comput. Biol., 6 (2010), pp. e1000890, 12, [https://doi.org/](https://doi.org/10.1371/journal.pcbi.1000890)  
 441 [10.1371/journal.pcbi.1000890](http://dx.doi.org/10.1371/journal.pcbi.1000890), <http://dx.doi.org/10.1371/journal.pcbi.1000890>.
- 442 [20] J. SARAGOSTI, V. CALVEZ, N. BOURNAVEAS, B. PERTHAME, A. BUGUIN, AND P. SILBERZAN, *Directional*  
 443 *persistence of chemotactic bacteria in a traveling concentration wave*, Proceedings of the National  
 444 Academy of Sciences, 108 (2011), pp. 16235–16240, <https://doi.org/10.1073/pnas.1101996108>, [http://](http://www.pnas.org/content/108/39/16235.abstract)  
 445 [www.pnas.org/content/108/39/16235.abstract](http://www.pnas.org/content/108/39/16235.abstract), <https://arxiv.org/abs/http://www.pnas.org/content/108/>  
 446 [39/16235.full.pdf+html](http://www.pnas.org/content/108/39/16235.full.pdf+html).
- 447 [21] S.JIN, *Asymptotic preserving (AP) schemes for multiscale kinetic and hyperbolic equations: a review*, Riv.  
 448 Mat. Univ. Prama, 3 (2012), pp. 177–216.
- 449 [22] S.JIN, L.PARESCHI, AND G.TOSCANI, *Uniformly accurate diffusive relaxation schemes for multiscale transport*  
 450 *equations*, SIAM J. NUMER.ANAL., 38 (2000), pp. 913–936.
- 451 [23] K. XU, *A gas-kinetic BGK scheme for the Navier-stokes equations and its connection with artifi-*

- 452        *cial dissipation and Godunov method*, Journal of Computational Physics, 171 (2001), pp. 289–335,  
453        <https://doi.org/http://dx.doi.org/10.1006/jcph.2001.6790>, [http://www.sciencedirect.com/science/article/  
454        pii/S0021999101967907](http://www.sciencedirect.com/science/article/pii/S0021999101967907).
- 455 [24] K. XU AND J.-C. HUANG, *A unified gas-kinetic scheme for continuum and rarefied flows*, Journal of Compu-  
456        tational Physics, 229 (2010), pp. 7747–7764, <https://doi.org/http://dx.doi.org/10.1016/j.jcp.2010.06.032>,  
457        <http://www.sciencedirect.com/science/article/pii/S0021999110003475>.